



LAWRENCE  
LIVERMORE  
NATIONAL  
LABORATORY

# ZnSe immersion grating in the short NIR region

Y. Ikeda, N. Kobayashi, P. J. Kuzmenko, S. L. Little, P. B. Mirkarimi, J. B. Alameda, S. Kaji, Y. Sarugaku, C. Yasui, S. Kondo, K. Fukue, H. Kawakita

July 9, 2014

Advances in Optical and Mechanical Technologies for  
Telescopes and Instrumentation  
Montreal, Canada  
June 22, 2014 through June 27, 2014

## **Disclaimer**

---

This document was prepared as an account of work sponsored by an agency of the United States government. Neither the United States government nor Lawrence Livermore National Security, LLC, nor any of their employees makes any warranty, expressed or implied, or assumes any legal liability or responsibility for the accuracy, completeness, or usefulness of any information, apparatus, product, or process disclosed, or represents that its use would not infringe privately owned rights. Reference herein to any specific commercial product, process, or service by trade name, trademark, manufacturer, or otherwise does not necessarily constitute or imply its endorsement, recommendation, or favoring by the United States government or Lawrence Livermore National Security, LLC. The views and opinions of authors expressed herein do not necessarily state or reflect those of the United States government or Lawrence Livermore National Security, LLC, and shall not be used for advertising or product endorsement purposes.

# ZnSe immersion grating in the short NIR region

Yuji Ikeda<sup>a,b</sup>, Naoto Kobayashi<sup>c</sup>, Paul J. Kuzmenko<sup>d</sup>, Steve L. Little<sup>d</sup>, Paul B. Mirkarimi<sup>d</sup>, Jennifer B. Alameda<sup>d</sup>, Sayumi Kaji<sup>e</sup>, Yuki Sarugaku<sup>f</sup>, Chikako Yasui<sup>g</sup>, Sohei Kondo<sup>b</sup>, Kei Fukue<sup>g</sup>, and Hideyo Kawakita<sup>e</sup>

<sup>a</sup>Photocoding, 460-102 Iwakura-Nakamachi, Sakyo-ku, Kyoto 606-0025, Japan;

<sup>b</sup>Koyama Astronomical Observatory, Kyoto-Sangyo University, Motoyama, Kamigamo, Kita-ku, Kyoto 606-8555, Japan;

<sup>c</sup>Institute of Astronomy, the University of Tokyo, 2-21-1 Osawa, Mitaka, Tokyo 181-0015, Japan;

<sup>d</sup>Lawrence Livermore National Laboratory, L-183 PO Box 808, Livermore, CA 94551;

<sup>e</sup>Department of Physics, Faculty of Science, Kyoto-Sangyo University, Motoyama, Kamigamo, Kita-ku, Kyoto 606-8555, Japan;

<sup>f</sup>Institute of Space and Astronautical Science, Japan Aerospace Exploration Agency, 3-1-1 Yoshinodai, Chuo-ku, Sagamihara, Kanagawa 252-5210, Japan;

<sup>g</sup>Department of Astronomy, Graduate School of Science, University of Tokyo, 7-3-1 Hongo, Bunkyo-ku, Tokyo 113-0033, Japan

## ABSTRACT

ZnSe has a high refractive index ( $n \sim 2.45$ ) and low optical loss ( $< 0.1/\text{cm}$ ) from 0.8 to 12  $\mu\text{m}$ . Therefore ZnSe immersion gratings can enable high-resolution spectroscopy over a wide wavelength range. We are developing ZnSe immersion gratings for a ground-based NIR high-resolution spectrograph WINERED. We previously produced a large prism-shaped ZnSe immersion grating with a grooved area 50 mm x 58 mm (Ikeda et al. 2010). However, we find two problems as NIR immersion grating: (i) serious chipping of the grooves, and (ii) inter-order ghosts in the diffraction pattern. We believed the chipping to be due to micro cracks just beneath surface present prior to diamond machining. Therefore we removed this damaged region, a few tens of microns thick, by etching the ZnSe grating blank with a mixture of HCl and HNO<sub>3</sub>. Ghosts appearing halfway between main diffraction orders originate from small differences in spacing between odd and even grooves. Apparently the blank shifts repeatably by about 120 nm in the direction orthogonal to the grooves depending on whether the translation stage holding the blank is moving right to left or left to right. Therefore we re-machined the grating only cutting grooves with the stage moving from right to left. After re-cutting, we also deposit the Cu coating with an enhanced interface layer of SiO<sub>2</sub> on the groove, which is developed in our previous study. We evaluated the optical performances of this immersion grating. It shows light scattering of 3.8 % at 1  $\mu\text{m}$ , no prominent ghosts, and a spectral resolution of 91,200 at 1  $\mu\text{m}$ . However we measured an absolute diffraction efficiency of only 27.3% for TE and 25.9 % for TM waves at 1.55  $\mu\text{m}$ . A non-immersed measurement of the diffraction efficiency of the facet blazed near 20° exceeded 60%, much closer to theoretical predictions. We plan to carry out more tests to resolve this discrepancy.

**Keywords:** Infrared, Spectroscopy, High resolution, Immersion grating, Nano-technology

## 1. Introduction

A grating immersed in an optical material of high refractive index  $n$ , called an immersion grating, is a powerful tool for astronomical spectroscopy. An immersion grating can provide  $n$  times the spectral resolution or can reduce the instrument size by a factor of  $1/n$ , compared to a classical reflective grating (see Figure.1 and equation (1) in Ikeda et al. 2008<sup>[1]</sup>). This type of grating attracted much interest as a key component for high resolution spectrographs with  $\lambda/\Delta\lambda > 70,000$  attached to extremely large telescopes such as the Thirty Meter Telescope. It also has value is moderate

resolution spectrographs ( $\lambda/\Delta\lambda > 30,000$ ) deployed on space telescopes because of the significant reductions in size as well as in weight and power consumption enabled by immersion.

WINERED is a near IR high resolution spectrograph attached to the 1.3m Araki Telescope of Koyama Astronomical Observatory (e.g., Ikeda et al. 2006<sup>[2]</sup> and Yasui et al. 2008<sup>[3]</sup>). An extremely high resolution mode with  $\lambda/\Delta\lambda_{\text{max}}=100,000$  in the z, Y, and J bands is under development using a ZnSe or ZnS immersion grating. We produced a large prism-shaped ZnSe immersion grating with an entrance aperture of 23 mm x 50 mm, a groove pitch of 30  $\mu\text{m}$ , and a blaze angle of 70 degree (Ikeda et al. 2010<sup>[4]</sup>, hereafter IK10), using nano precision fly-cutting machine (PERL) at the Lawrence Livermore National Laboratory which is developed for achieving Ge immersion grating (Kuzmenko et al. 2006<sup>[5]</sup>). From our detailed evaluation on the optical performance, we discovered two issues: (i) there is much chipping at the groove edge, resulting in a large amount of scattered light and (ii) significant ghosts halfway between orders appear in the diffraction pattern. We believe that the chipping is due to subsurface damage present in the grating blank, and that the ghosting is due to differences in groove pitch between odd and even lines produced by bi-directional cutting (see IK10).

We solved these problems during the past few years and fabricated an improved ZnSe immersion grating. It has a special reflective metal coating on the grooves, which we have developed along with the cutting technique reported in IK10. In this paper, we report the technical details of the fabrication (in section 2) and the optical performances (in section 3).

## **2. Fabrication of prism ZnSe immersion grating**

### **2.1 Surface preparation of the ZnSe grating blank**

LLNL has had very good success in machining high quality gratings in germanium (e.g., Kuzmenko et al. 2006<sup>[5]</sup>), but our ability to cut good gratings in zinc selenide not been as consistent (Kuzmenko et al. 2010<sup>[6]</sup>). If the diamond tool has been properly shaped, is in good condition and the machining parameters are correctly chosen, then excess chipping is most likely caused by subsurface damage present in the grating blank. Microcracks in the surface resulting from previous fabrication steps (e.g. grinding and polishing) cause the material to break along cracks rather than along the direction of tool motion.

Our germanium blanks receive a polishing etch before machining that removes the outermost 50  $\mu\text{m}$  from all surfaces. Unfortunately the technology for etching ZnSe is not at all as well developed as that for germanium, which has had a long history of use in the semiconductor industry. It is possible to polish a damage-free surface in ZnSe as some of our positive results have shown (see Kuzmenko et al. 2010<sup>[6]</sup>). But inconsistencies between vendors and sometimes over time with the same vendor led us to seriously explore the possibility of etching our ZnSe blanks before machining.

There are a number of papers and patents on ZnSe etchants in the literature (e.g., Gavrishchuk et al. 2007<sup>[7]</sup> and Lucca et al. 2004<sup>[8]</sup>). We tested them on some spare ZnSe windows. A dab of optical wax (mix of beeswax and rosin) was used to mask off part of the surface from the etchant in order to measure the etch rate. The first test using concentrated HCl only removed 2  $\mu\text{m}$  in 60 minutes, so a more aggressive etchant was needed.

The second waxed ZnSe disc was placed in 1:1 mixture of HCl and HNO<sub>3</sub> for 60 minutes. It etched rapidly and left a discolored layer (possibly an oxide) that we removed with an additional 30 minute etch in concentrated HCl (see Figure 1). The etch depth measured by profilometry was 42  $\mu\text{m}$ , but there was a trench of about 245  $\mu\text{m}$  that can be seen in the photo around the perimeter of the wax boundary. This may have been a kinetic effect as the etchant was not stirred. However, the removal of 40  $\mu\text{m}$  of material was sufficient to have eliminated subsurface damage. We cut a test grating and obtained minimal chipping of grooves over both the etched and unetched regions of the disc. This apparently meant that the disc had received a very good polish and was damage-free even before etching.

We prepared the large prism by coating all but the hypotenuse with wax (the existing grating had been previously polished off). It was etched for 1 hour in a continuously stirred 700 ml of a 1:1 mixture of HCl and HNO<sub>3</sub>. The surface was still quite transparent after etching although it appeared textured in reflected light. The etch was fairly uniform but there remained some pitting out near the edges.

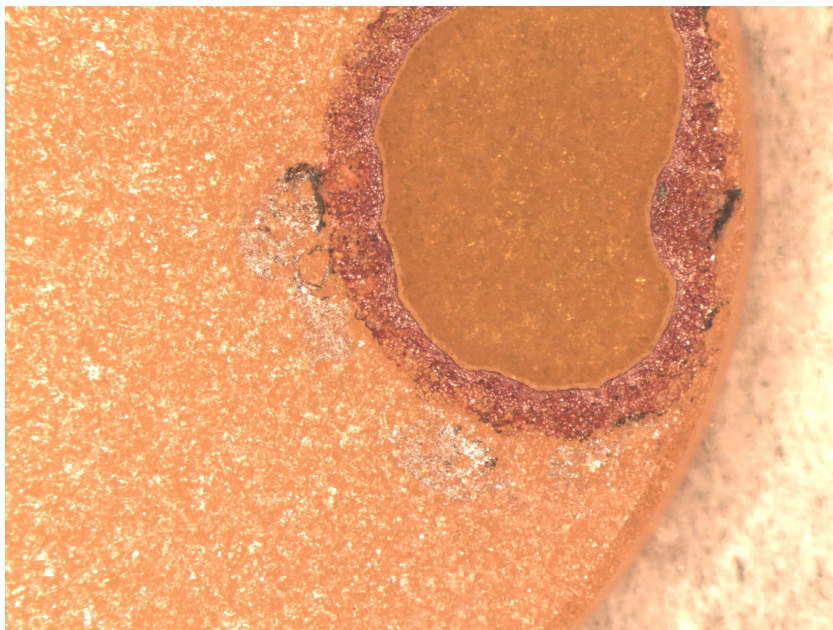


Figure 1: Results of 60 minute etch of ZnSe window in 1:1 of HCl:HNO<sub>3</sub>, followed by 30 minutes in concentrated HCl.

## 2.2 Machining the grating

The presence of ghosts exactly halfway between the main diffraction peaks, seen in the previous trial reported in IK10, implies a periodic error in groove position with a period of two grooves. In a system where groove position is interferometrically controlled this should not occur. A close examination of the PERL structure shows that position of the spindle, which cuts the grooves, is interferometrically controlled with respect to a reference mirror mounted to the granite machine base. But it is not interferometrically controlled with respect to the x-slide upon which the grating blank rests. Gratings are currently cut with a back and forth (= bi-directional) motion, such that the x-slide alternates left and right motion between increments of the spindle position as grooves are cut. If there is a very slight (few nm) shift in the z-direction of the x-slide depending on the direction of motion, it could cause the observed ghosting.

In March 2012 an experiment was performed comparing 5 mm of grooves cut with the standard back and forth motion with 5 mm of grooves cut on the same ZnSe substrate using unidirectional cutting (i.e. grooves were cut only while the x-stage was moving to the right). We used a ZnSe disc that had previously been etched to remove subsurface damage. Examination of diffraction patterns with a HeNe laser showed the presence of ghosts in the bidirectional cut grooves but none down to the limit of our measurement in the unidirectionally cut grooves. This procedure would be followed in machining the prism grating.

We began by machining a test grating in germanium to test the diamond tool and to verify the blaze angle. We had hoped for a 70 degree blaze as that would put the grating facets approximately parallel to the entrance face of the prism and assure that the peak of each diffraction would exit parallel to the base of the prism. Unfortunately the angles of the two facets measured 67.27 degree and 17.57 degree. Note that the angle at the base of the grooves is 84.8 degree and not 90 degree. It is possible to make a small adjustment in the blaze angle by grinding away on the metal shank of the diamond tool so that the tool shank and therefore the diamond tip are slightly angled when fastened into the tool holder. This was done and another test grating was machined to check the results of the adjustment. This test grating would also be a dry

run for machining the prism so we chose an identical grating pitch of  $31.7\text{ }\mu\text{m}$ . The blank was a  $12 \times 12 \times 1\text{ mm}$  ZnSe window. It never had been machined before so we expected low subsurface damage. The blank was waxed down to steel parallel and mounted in PERL. We used machining conditions identical to those planned for the prism: 1000 rpm on the spindle and 0.35 inch/minute feed rate. Cutting was unidirectional to eliminate ghosts. The direction of feed was into the direction of rotation of the diamond tool. This technique, known as climb cutting, produces the best surface finish. The machining took nearly 24 hours. When finished the grating was removed from the machined and cleaned with a strippable coating to remove particulate residue. The blaze was measured to be  $69.64\text{ degree}$  (see section 3.1 on the method of measurement) and there were no discernable ghosts in the diffraction pattern. Figure 2 shows an interferometric measurement of the surface figure. The thinness of the blank contributes to the relatively large surface error.

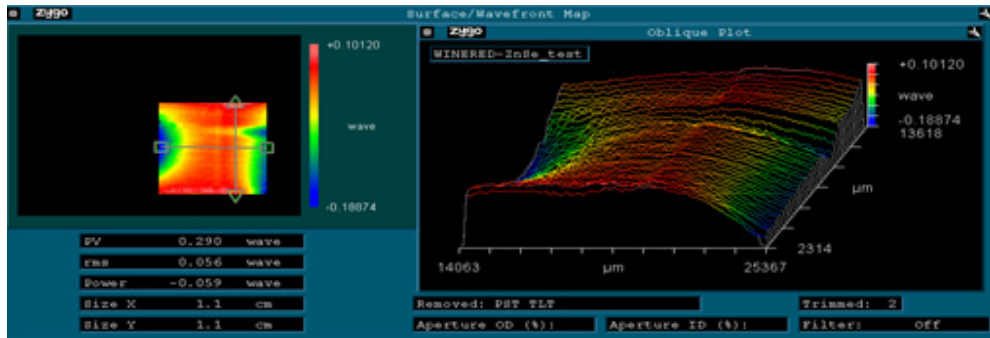


Figure 2. Interferometric measurement of surface error on test grating cut into  $12 \times 12\text{ mm}$  ZnSe. The measurement may actually be on the  $20\text{ degree}$  facet.

The left of Figure 3 shows the installation of the prism blank into its machining fixture where it is secured by cyanoacrylate adhesive. Due to the thickness of the blank the one inch thick steel mounting plate on the translation stage had to be removed to fit the machining fixture beneath the diamond tool (see the right of Figure 3). An 18 hour thermal soak was performed to bring the entire machine to equilibrium. This was done with the spindle rotating but not cutting the blank. Cutting began at 9 AM on Oct.10 in 2012 and was expected to last about 14 days. Unfortunately a momentary dip in supplied electrical voltage (brownout) extending across most of LLNL caused the control computer to halt on the morning of Oct. 19. Roughly  $40\text{ mm}$  of the  $58\text{ mm}$  length grating had been cut. Since knowledge of absolute tool position was lost it was impossible to restart the cut from where it had stopped. The grating was removed from machine and cleaned in preparation for testing. Figure 4 shows the grooves at  $200\times$  magnification with the microscope. There is a small amount of chipping but in general the grooves look satisfactory.

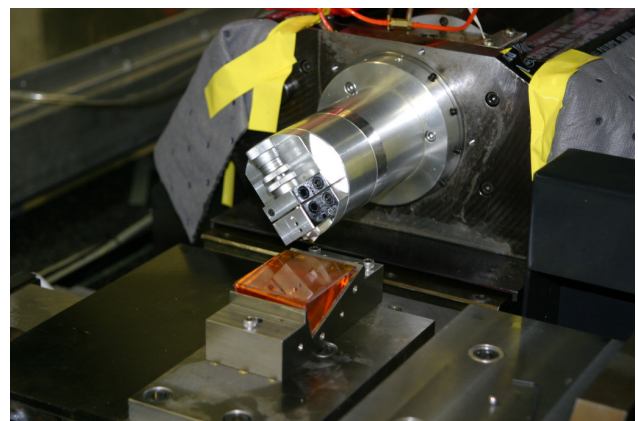
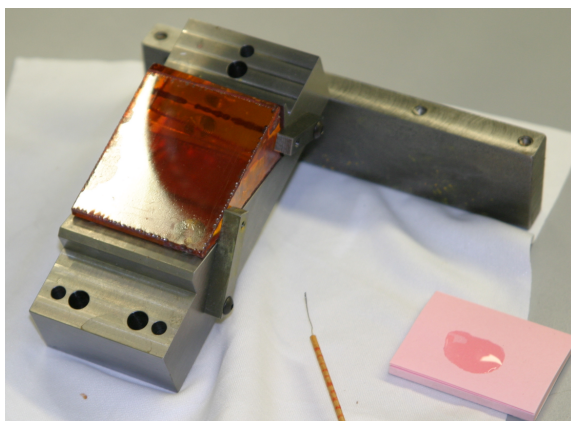


Figure 3. ZnSe grating blank installed in machining fixture (left). Cyanoacrylate adhesive is left to cure overnight for best chemical resistance. Grating blank installed in PERL and ready to cut (right).





Figure 4. Photo of the grooves at 200x magnification. You can see some particulate residue that I will remove later with the strippable coating cleaner. Some of that may be subsurface damage.

### 2.3 Metal coating on the grooves

Immersion gratings require high reflectivity coatings on the grooves in order to achieve high optical efficiency. In IK10 we demonstrated a multilayer coating that yielded a reflectivity of greater than 90% over the spectral region of interest (0.9 to 1.3  $\mu\text{m}$ ) when deposited onto flat ZnS and ZnSe substrates. This coating consisted of 130 nm of  $\text{SiO}_2$  followed by 200 nm of Cu (providing the reflectivity) and a 5 nm SiC capping layer to prevent copper degradation due to atmospheric exposure. The  $\text{SiO}_2$  serves two functions. First it acts as a barrier to prevent a chemical reaction between the copper and the sulfur or selenium in the substrate. This reaction is responsible for the reduced reflectivity observed when copper is deposited directly onto the substrates. Secondly the low index of the  $\text{SiO}_2$  results in a higher reflectivity from the  $\text{SiO}_2$ –Cu interface than from a ZnSe–Cu interface. An additional reflection occurs at the ZnSe– $\text{SiO}_2$  interface, which by choice of the proper  $\text{SiO}_2$  thickness adds in phase with the reflection at the  $\text{SiO}_2$ –Cu interface.

In January 2011 this coating was deposited on one-inch diameter polished ZnSe and ZnS windows. The spectral reflectance was measured at that time and again in May 2012 after storage in the telescope dome of the Koyama Astronomical Observatory of Kyoto-Sangyo University in Kyoto, Japan. Kyoto has a humid climate. The relative humidity of the telescope dome ranges from 80% to 90% in summer, which is an appropriate condition for the environment testing of the coating. There was no observable change in the immersed reflectivities. These measurements were repeated in May 2014 and as seen in Figure 5. There is no degradation of the reflectivity within the uncertainty of the measurement. This demonstrates that the coating is robust and stable in a telescope environment.

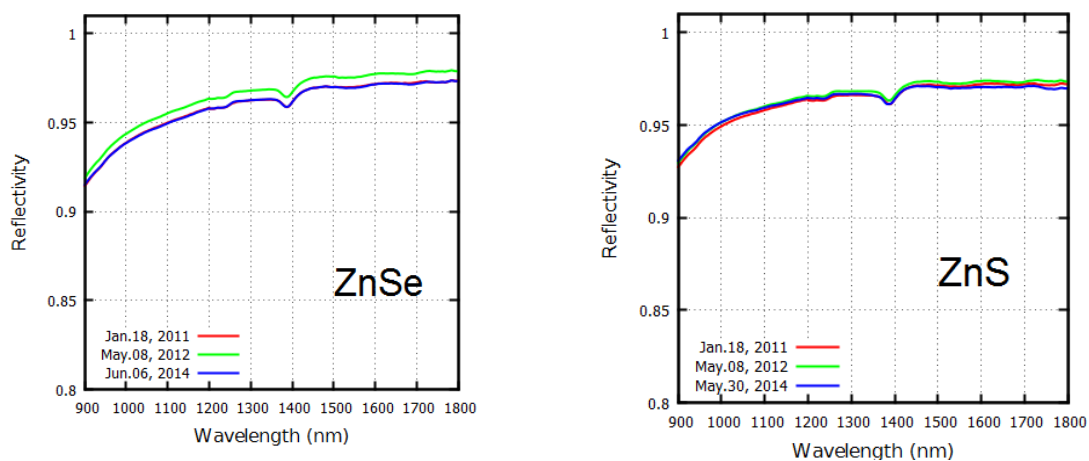


Figure 5: Variation of immersed reflectance of  $\text{SiO}_2$ –Cu coating on ZnSe (left) and ZnS (right) substrates during three years.

The coating clearly works well on flat immersed mirrors but it was uncertain if it could be deposited on a grooved surface and how well it would perform on an actual immersion grating. A major concern was the steep 70 degree angle of inclination of the surfaces to be coated. Metallic coatings deposited at near 90 degree inclination can be quite rough due to shadowing effects as the coating material is laid down. Leem et al. (2013)<sup>[9]</sup> reported porous films with reduced refractive index in glancing angle deposition (80 degree angle). The first step was to calibrate the deposition rates of SiO<sub>2</sub> and Cu on inclined substrates in the LLNL Mag 1 magnetron sputtering system. We mounted pieces of silicon wafers in the coater at normal incidence and at a 70 degree inclination. Copper and SiO<sub>2</sub> were deposited in separate runs. The film thicknesses were measured by x-ray reflectivity. We found the thickness on the 70 degree inclined surface to be about 65% that at normal incidence. A laser reflected from the surface of the samples showed no unusual scatter so the roughness of the deposited films was acceptable. Next we measured the spectral reflectivity of the SiO<sub>2</sub> on silicon. A porous coating will have a lower index than bulk material. We compared the measured reflectivity to that calculated from the known thickness and from tabulated values of the refractive index of amorphous SiO<sub>2</sub>. The agreement was very good indicating that the index of silica is unchanged when deposited at 70 degree (i.e. no porosity in the coating).

Before applying our high reflectance coating the large prism grating we tested it on a smaller grating previously machined on one half of a one-inch diameter ZnSe substrate. The grating had a pitch of 30  $\mu\text{m}$  and a blaze angle of about 62 degree. A cleaved silicon wafer was used to mask off half of the grating so that a direct comparison could be made between the reflections from a coated and an uncoated section of the same grating. A photo of the coated disc grating can be seen on the left side of Figure 6. Due to the high index of the ZnSe it is not possible to illuminate the steeply angled grooves from the back surface of the disc. Instead a special entrance face needed to be created as shown in the center of Figure 6. The complete polished prism is shown in the right side photo of Figure 6. I illuminated the steeply angle grooves with a HeNe laser to test the grating in immersion. The pattern from the copper coated area was the same as the uncoated area only brighter. Quantitative tests with a power meter showed that the ratio of the reflectivity of the coated to the uncoated grooves was about 5.5. This seems high. But since the overall results were good we had confidence to apply the coating to the large prism grating.

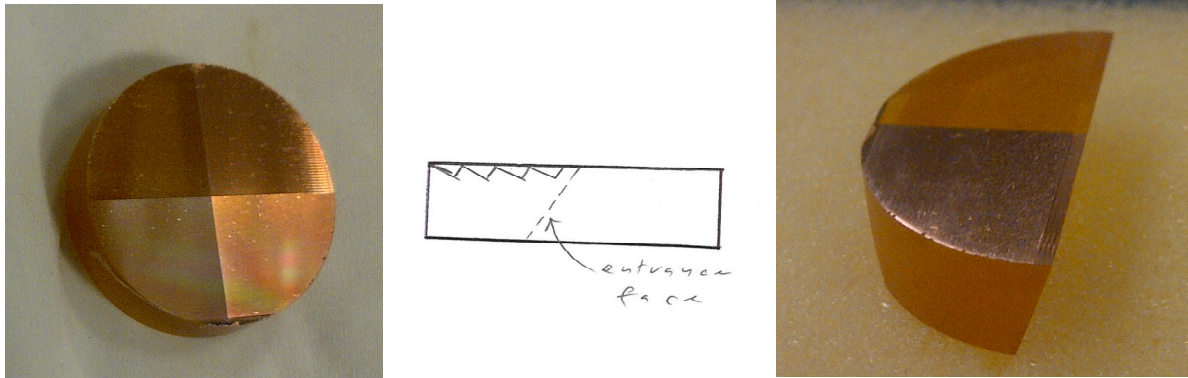


Figure 6: Left image shows a reflective coating (130 nm SiO<sub>2</sub>/200 nm Cu/5 nm SiC) deposited on half of a one inch diameter ZnSe disc into which a grating had previously been machined. Center image shows how the disc will be cut into a prism shape to allow optical access to the 70 degree blazed facets. Right image shows finished prism

Unlike the disc grating which had 2 parallel surface and could be clamped flat in the coater, the triangular shape of the large prism grating required the fabrication of a special fixture to hold it in the coating chamber. The fixture with the prism in place can be seen in the left of Figure 7. The reflective coating was deposited over the full surface of the prism hypotenuse except for a small area around the periphery where it was covered by the edges of the holder. The prism grating after coating can be seen in the right of Figure 7.



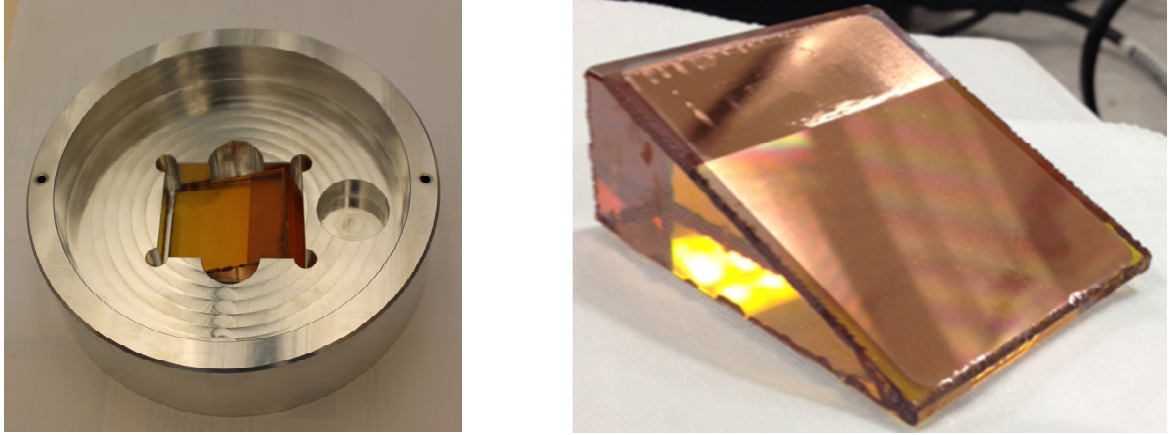


Figure 7. The ZnSe prism with the grating facing downward is mounted in the coating fixture (left) and prism grating after coating deposition (right). The lower reflective region of the diffraction surface form to grating (The remaining upper region is not machined because of the halt cutting by a transient dip in electrical power. See text in more details).

### 3. Optical performances

We evaluated the optical performances of the fabricated ZnSe immersion grating. The optical requirements of the ZnSe immersion grating are summarized in Table 1. These requirements are determined by the optical design of WINERED.

Table 1: Summary of optical specifications of ZnSe immersion grating for WINERED

items	blaze angle	surface irregularity	ghost intensity	Absolute diffraction efficiency	spectral resolution
specification	$70 \pm 0.3$ deg.	$1.0 \lambda$ at 633nm (PV) $0.071 \lambda$ at 633nm (rms)	$< 0.1\%$	$> 70\%$ at $1 \mu\text{m}$	$> 100,000$ at $1 \mu\text{m}$

#### 3.1 Blaze angle

We measured the blaze angle using the method shown in Figure 6.8 of Loewen & Popov (1997)<sup>[10]</sup>. A HeNe laser is directed at the grooves from the air side of the grating (non-immersed) and the diffraction pattern is observed. The intensity ratio between the strongest order ( $m=89$ ) and the next strongest order ( $m=90$ ) is  $I_{2nd}/I_{1st} = 0.474$ . The diffraction angles of these orders are  $\theta_{1st}=68.8$  degree and  $\theta_{2nd}=70.4$  degree, respectively. We obtained a blaze angle  $\theta_b=69.3 \pm 0.3$  degree from the following equation.

$$\sin \theta_B = \frac{I_{1st} \sin \theta_{1st} + I_{2nd} \sin \theta_{2nd}}{I_{1st} + I_{2nd}} \dots (1)$$

#### 3.2 Surface irregularity

Figure 8 shows the surface irregularity measured in immersion using a Zygo interferometer at 633 nm. The diffraction order is  $m=230$ . The measured irregularity includes the inhomogeneity of the refractive index of ZnSe, but this expected to be small. The measured error at 633 nm is equivalent to  $0.84\lambda$  (PV) and  $0.16\lambda$  (rms) at  $1.0 \mu\text{m}$ , which almost satisfy the WINERED specification (see Table 1). However, we can see wave-like profiles with the high frequency greater than 1.0 lines/mm and the small amplitude less than  $0.1\lambda$  along the groove direction, which could degradation the diffraction efficiency and the spectral resolution (see section 3.5).

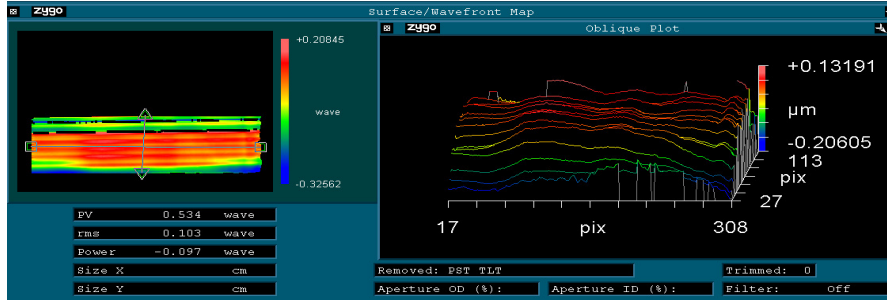


Figure 8: Interferometric measurement of surface irregularity of ZnSe prism grating seen in immersion configuration.

### 3.3 Ghost and pitch error

Figure 9 shows the diffraction pattern of a HeNe laser in the immersion configuration. This spectrum, in which the two strongest orders and the scattered light in the inter orders is seen, is obtained with a two dimensional cooled CCD camera. At first glance, the intermediate ghost at the middle of the order is greatly reduced compared to the sample reported in IK10. This suggests that mono-directional cutting reduces effectively a component with the harmonic overtone of the groove pitch, which would be imprinted by a bi-directional cutting. However, the small grass ghosts which spread all over the inter-order region are still seen with the maximum intensity of 0.1%. They might be related to the wave-like profile along the grooves seen the interferometric result on the diffraction surface in the previous subsection. The intensity of the inter-order scattered light,  $I_{sca}/I_0$ , is 10.2% at 633 nm. This originates from the random pitch error of the groove and does not include the bulk scattering in ZnSe as reported by Ikeda et al. (2009)<sup>[11]</sup> and the scattering by the surface roughness of the groove facet. These components already have been subtracted as the background light on the CCD detector because their intensity is distributed not only in the dispersion direction but also the spatial direction. Therefore, we can estimate the random pitch error  $\sigma_d$  with the measured intensity of the scattered light and the following equation,

$$\sigma_d = \frac{\lambda}{4\pi n \sin \theta_B} \sqrt{\frac{I_{sca}}{I_0}} \dots (2)$$

Using  $\lambda=633$  nm,  $n=2.59$ ,  $\theta_B=70$ deg, and  $I_{sca}/I_0 = 10.2\%$ , we estimate the random pitch error  $\sigma_d=6.6$ nm (rms). By contraries, we can estimate the scattering loss by the random pitch error at aimed wavelengths with the same equation (2). The estimated scattering losses are 3.8% at  $1\mu\text{m}$  and 1.6% at  $1.5\mu\text{m}$  in the immersion configuration, respectively.

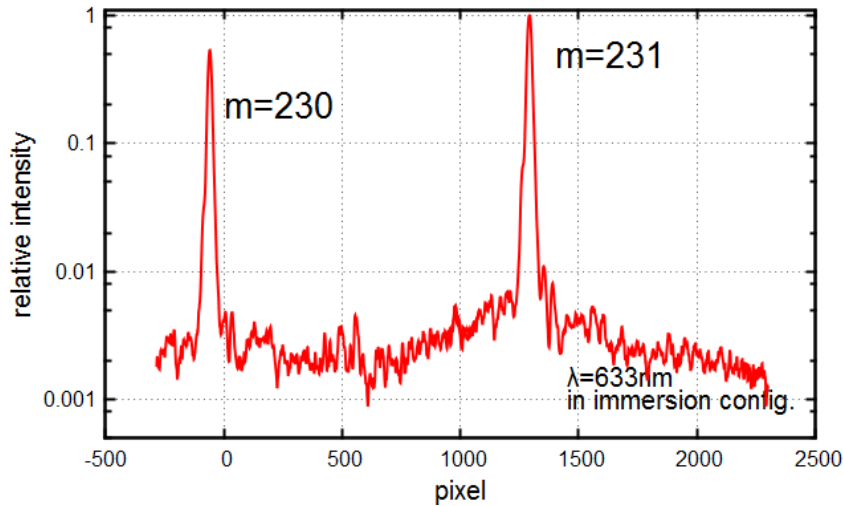


Figure 9. The obtained diffracted spectrum in an immersion configuration at 633 nm. We can see the inter-order scattered light at the level of  $10^{-3}$ . This would originate from the random pitch error. The ghost intensity is less than 0.1%. See text in more detail.

### 3.4 Diffraction efficiency

We measured the absolute diffraction efficiency around  $1.55\ \mu\text{m}$  using a tunable diode laser. The configuration of the test optics is shown in Figure 10. The IR light from the tunable laser is coupled into a single mode PMF (=polarization maintaining fiber) and collimated by a lens. After the polarization angle of the collimated beam is adjusted with a half wave plate, the beam reduced to 5mm by the variable diaphragm aperture enters the immersion grating. The diffracted light is focused on the two dimensional InGaAs array by the IR camera lens. By measuring the total flux at each wavelength, we can estimate the absolute diffraction efficiency. To correct for time variation of laser power, we simultaneously measure power in a reference beam together with power in the diffracted beam (see Figure. 10). We correct for the reflection losses at the entrance/exit surface by calculating a reflectivity based on the refractive index of ZnSe at  $1.55\ \mu\text{m}$  ( $n=2.46$ ).

Figure 11 shows absolute diffraction efficiencies for TE and TM waves. We also plot the diffraction efficiencies predicted with RCWA (=Rigorous Coupled-Wave Analysis) method for a model including the  $\text{SiO}_2$ , Cu, and SiC thin films described in section 2.2. Although the model calculation predicts efficiencies of 72.1% for TE wave and 73.9% for TM wave, measured efficiencies are only 27.3% for TE and 25.9% for TM. The predicted diffraction efficiencies do not include the scattering and/or absorption loss by the random pitch error ( $=1.6\%$  at  $1.55\ \mu\text{m}$ , see section 3.3), the surface roughness on the groove facet ( $=1.1\%$  at  $1.55\ \mu\text{m}$ ), and the internal attenuation ( $=8.3\%$  at  $1.55\ \mu\text{m}$  which is estimated from the measurements by Ikeda et al. 2009<sup>[11]</sup>). Even taking these degradations into consideration, the predicted peak efficiencies become 66.0% for TE and 64.4% for TM, which are larger than the measured ones by a factor of 2.5.

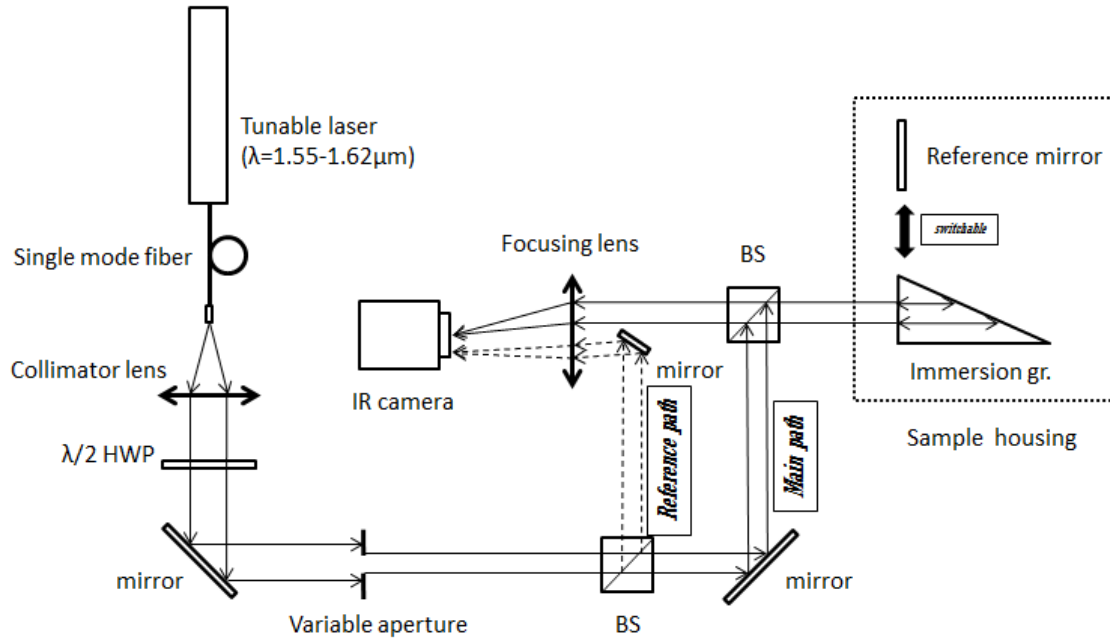


Figure 10. The optical configuration of an instrument for measuring the diffraction efficiency in the IR region.

There are a few possibilities for explaining this inconsistency. One is coating imperfections on the diffracting surface, another is the deviation of the groove shapes from an ideal rectangle profile. To investigate these possibilities, we measured the diffraction efficiency of the 70 degree blazed facets in the non-immersed configuration using a HeNe laser. The diffraction energy concentrating on the central two orders is obtained to be only 13%, although a RCWA simulation predicts 65%. This suggests that the poor diffraction efficiency in immersion configuration does not originate from the coating process but the machining process. In addition,, we also measured the diffraction efficiency (non-immersed) of the nominally 20 degree blazed facets (actual blaze was near 15 degrees) and obtained values of greater than 60% at 633nm, which is much close to the predicted efficiencies. This result supports the hypothesis that the poor diffraction efficiency is related to the machining process, because shallow blazed facets are less sensitive to errors than steeply blaze

facets. If the groove facet would be tilted, has a concave/convex shape or a round at the top or the valley of the groove, and so on, the peak efficiency becomes to decrease compared to the theoretical prediction and the diffracted energy is distributed into the neighboring other orders (widely spread in space). Indeed, the wavelength dependence of the diffraction efficiency is not peaky but relatively flat (see Figure 11).

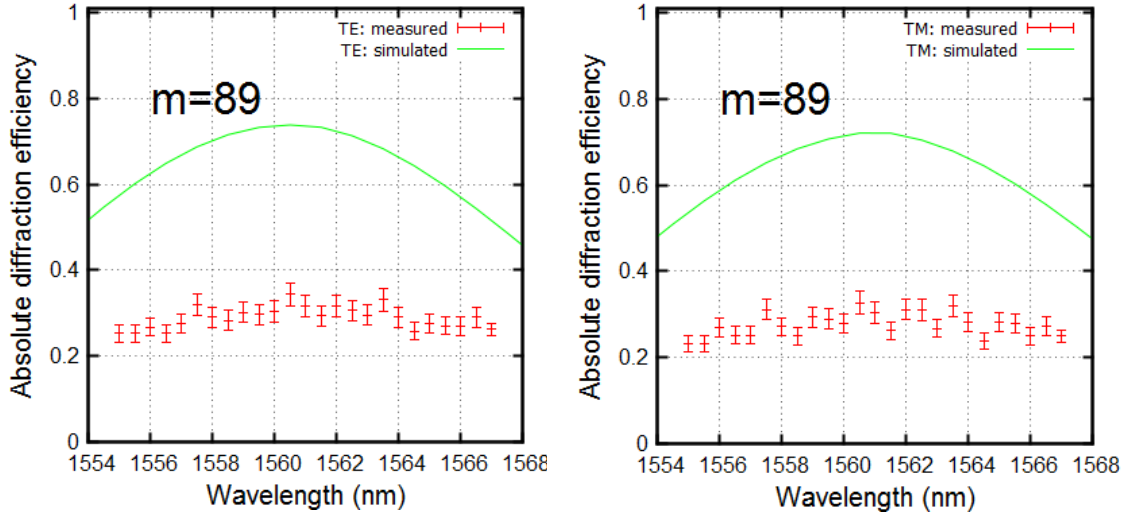


Figure 11. The measured absolute diffraction efficiencies of the ZnSe immersion grating for TE (left) and TM waves (right). The solid curves are simulated efficiencies with RCWA method (see text in more details).

### 3.5 Spectral resolution

We can obtain a monochromatic PSF in the immersion configuration by two dimensional Fourier transform of the wavefront error map shown in Figure.8. In addition, we obtain the LSF (=Line Spread Function) by convolving it in the dispersion direction (see Figure 12). The profile is roughly symmetry and very sharp, but we can see a small bump in the left side lobe. This is generated by small wave-like roll profiles along the groove seen the wavefront map. The maximum spectral resolution, which can be estimated from the FWHM of this LSF, is  $\lambda/\Delta\lambda=91,200$  at  $1\text{ }\mu\text{m}$ . Note that the theoretical maximum resolution of this grating is designed as  $\lambda/\Delta\lambda=112,000$ .

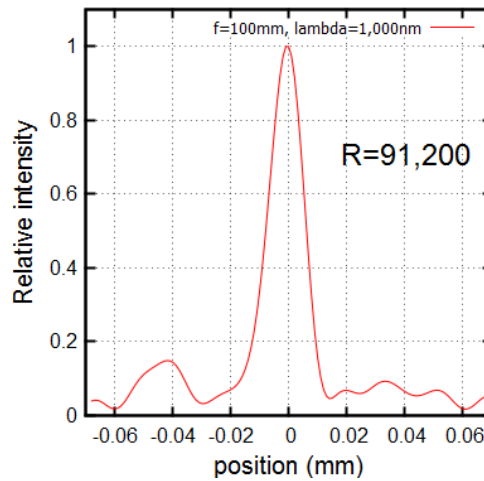


Figure 12. The normalized line spread function with the aperture size of 8.2mm at  $1.0\text{ }\mu\text{m}$ .

#### 4. Summary

We are developing ZnSe immersion gratings for the next generation NIR and Mid-IR high resolution astronomical spectrographs. There were two problems reported with the prism shaped ZnSe immersion grating which we fabricated in IK10: significant chipping at the groove edge and noticeable ghosts between of orders. In this paper, we overcame these problems by establishing a method for removing the subsurface damage in the ZnSe blank and adapting a new machining process (unidirectional cutting). Using these techniques, we realized the first prism-shaped ZnSe immersion grating with a reflective copper coating (also developed in IK10) on the grooves. This ZnSe immersion grating shows mostly good optical performance: low light scattering of 3.8% at 1 $\mu$ m, no prominent ghosts, and a high spectral resolution of 91,200 at 1  $\mu$ m. However the diffraction efficiencies were poor at 1.55  $\mu$ m (27.3% for TE and 25.9% for TM waves). This poor diffraction efficiency appears to originate from the machining process. We will carry out the additional tests to resolve this discrepancy.

#### ACKNOWLEDGMENTS

We would like to thank T. Sukegawa of CANON Inc. and H. Kobayashi of Kyoto-Nijikoubou LLP. for supporting our measurement and the data reduction on the diffraction efficiency of the grating, respectively. We also would like to thanks all staff of Koyama Astronomical Observatory of Kyoto-Sangyo University for various supports and help in this program. This study was supported by KAKENHI(16684001) Grant-in-Aid for Young Scientists (A), KAKENHI(20340042) Grant-in-Aid for Scientific Re-search (B), and KAKENHI(21840052) Grant-in-Aid for Young Scientists (Start-up), by Japan Society for the Promotion of Science. Lawrence Livermore National Laboratory is operated by Lawrence Livermore National Security, LLC, for the U.S. Department of Energy, National Nuclear Security Administration under Contract DE-AC52-07NA27344.

#### REFERENCES

- [1] Ikeda, Y., Kobayashi, N., Kuzmenko, P., Little, S., Yasui, C., Kondo, S., Minami, A., and Motohara, K., "Diamond-machined ZnSe immersion grating for NIR high-resolution spectroscopy," in [*Advanced Optical and Mechanical Technologies in Telescopes and Instrumentation. Proceedings of the SPIE, 7018-183*], Presented at the Society of Photo-Optical Instrumentation Engineers (SPIE) Conference **7018** (June 2008).
- [2] Ikeda, Y., Kobayashi, N., Kondo, S., Yasui, C., Motohara, K., and Minami, A., "WINERED: a warm near-infrared high-resolution spectrograph," in [*Ground-based and Airborne Instrumentation for Astronomy. Edited by McLean, Ian S.; Iye, Masanori. Proceedings of the SPIE, Volume 6269, pp. 62693T (2006).*], Presented at the Society of Photo-Optical Instrumentation Engineers (SPIE) Conference **6269**, 62693T (July 2006).
- [3] Yasui, C., Ikeda, Y., Kondo, S., Motohara, K., Minami, A., and Kobayashi, N., "Warm infrared Echelle spectrograph (WINERED): testing of optical components and performance evaluation of the optical system," in [*Ground-based and Airborne Instrumentation for Astronomy II. Proceedings of the SPIE, 7014-108*], Presented at the Society of Photo-Optical Instrumentation Engineers (SPIE) Conference **7014** (June 2008).
- [4] Ikeda, Y., Kobayashi, N., Kuzmenko, P. J., Little, S. L., Yasui, C., Kondo, S., Mito, H., Nakanishi, K., and Sarugaku, Y., "Fabrication and current optical performance of a large diamond-machined ZnSe immersion grating," in [*Society of Photo-Optical Instrumentation Engineers (SPIE) Conference Series*], Society of Photo-Optical Instrumentation Engineers (SPIE) Conference Series **7739**, 77394G (July 2010).
- [5] Kuzmenko, P. J., Davis, P. J., Little, S. L., Little, L. M., and Bixler, J. V., "High efficiency germanium immersion gratings," in [*Optomechanical Technologies for Astronomy. Edited by Atad-Ettinger, Eli; Antebi, Joseph; Lemke, Dietrich. Proceedings of the SPIE, Volume 6273, pp. 62733T (2006).*], Presented at the Society of Photo-Optical Instrumentation Engineers (SPIE) Conference **6273**, 62733T (July 2006).
- [6] Kuzmenko, P. J., Little, S. L., Ikeda, Y. and Kobayashi N., "Progress in the fabrication of a prototype ZnSe immersion grating for the WINERED spectrograph," in [*Society of Photo-Optical Instrumentation Engineers (SPIE) Conference Series*], Society of Photo-Optical Instrumentation Engineers (SPIE) Conference Series **7739**, 77393U (July 2010).

- [7] Gavrishchuk, E. M., Vilkova, E. Yu., Timofeev, O. V., Borovskikh, U. P. and Tikhonova, E. L., "Etching behavior of CVD zinc selenide in inorganic acid solutions," *Inorganic Materials* **43**(6), 579-583 (2007).
- [8] Lucca, D. A., Wetteland, C. J., Misra, A., Klopstein, M. J., Nastasi, M., Maggiore, C. J. and Tesmer, J. R., "Assessment of subsurface damage in polished II-VI semiconductors by ion channeling," *Nuclear Instruments and Methods in Physics Research B* 219-220, 611-617 (2004).
- [9] Leem, J. L. et al., "Single-material zinc sulfide bi-layer antireflection coatings for GaAs solar cells," *Optics Express* **21**(18), A821-A828 (2013).
- [10] Loewen, E. G. and Popov, E., [*Diffraction gratings and applications*], Diffraction gratings and applications by Erwin G. Loewen and Evgeny Popov. New York : M. Dekker, c1997. (1997).
- [11] Ikeda, Y., Kobayashi, N., Kondo, S., Yasui, C., Kuzmenko, P. J., Tokoro, H., and Terada, H., "Zinc sulfide and zinc selenide immersion gratings for astronomical high-resolution spectroscopy: evaluation of internal attenuation of bulk materials in the short near-infrared region," *Optical Engineering* **48**, 084001-+ (Aug. 2009).